Regrowth Interface Quality Dependence on Thermal Cleaning of AlGaInAs/InP Buried-Heterostructure Lasers

2011 Jpn. J. Appl. Phys. 50 070203

(http://iopscience.iop.org/1347-4065/50/7R/070203)

DOI: 10.1143/JJAP.50.070203

Regrowth Interface Quality Dependence on Thermal Cleaning of AlGaInAs/InP Buried-Heterostructure Lasers

Yuta Takino[1], Mizuki Shirao[1], Takashi Sato[1], Nobuhiko Nishiyama[1*], Tomohiro Amemiya[1,2], and Shigehisa Arai[1,2]

[1] *Department of Electrical and Electronic Engineering, Tokyo Institute of Technology, Meguro, Tokyo 152-8552, Japan*
[2] *Quantum Nanoelectronics Research Center, Tokyo Institute of Technology, Meguro, Tokyo 152-8552, Japan*

Received November 13, 2010; accepted April 7, 2011; published online July 5, 2011

The effect of *in-situ* thermal cleaning on the regrowth interface quality of 1.3 μm AlGaInAs/InP buried-heterostructure lasers prepared by organometallic vapor-phase epitaxy (OMVPE) was investigated. It was proven that the regrowth interface quality can be quantitatively evaluated on the basis of the surface recombination velocity determined from the electroluminescence property below the threshold, and the tendency of the characteristics agreed with the lasing properties. As a result of a successful operation with the stripe width of 3.6 μm, treated by the thermal cleaning process at a temperature of 450 °C for 30–60 min in a PH_3 atmosphere, an internal quantum efficiency of approximately 70% was achieved.

The AlGaInAs/InP alloy system is very attractive for achieving low-cost and low-power semiconductor laser modules for optical communications. This is due to the fact that it is suitable for thermoelectric-cooler-less operation,[1–3] because its conduction band offset ($\Delta E_c = 0.75\Delta E_g$) is larger than that of the GaInAsP/InP system ($\Delta E_c = 0.40\Delta E_g$).[4] This large conduction band offset leads good electron confinement and differential gain even at high temperature operation range.[5,6] In addition, in optical fiber communication applications, buried-heterostructure (BH) lasers have been adopted over lasers with a ridge structure because of their advantages such as low operation current, stable output beam pattern, and high-speed operation.[7–9] Thus, the combination of the material system and the structure has good potential as high performance lasers.[9–12]

However, it is difficult to realize BH lasers based on the AlGaInAs/InP system since the Al-containing layers are easily oxidized during fabrication. The oxidation prevents high-quality crystal growth during embedding growth, resulting in not only poor lasing characteristics but also low reliability.[12] Therefore, a process for removing the oxidized Al-containing layers or prevent oxidation itself is required. Various methods have been investigated towards achieving this objective, for example, cleaning before regrowth,[7,8] adopting the narrow-stripe selective organometallic vapor-phase-epitaxy (NS-OMVPE) method,[9] and *in-situ* etching prior to regrowth.[13] The lasing, modulation and other characteristics of AlGaInAs/InP BH lasers subjected to these methods have been reported.[7–14] However, quantitative studies of the regrowth interface quality of BH structures have not been reported.

In this paper, we report the influence of *in-situ* thermal cleaning on the interface quality determined by evaluating the surface recombination rate at the regrowth interfaces from the electroluminescence slope efficiency below the threshold.

The structure of the fabricated AlGaInAs/InP BH laser is shown in Fig. 1. The initial wafer was grown on a (100) n-InP substrate by the OMVPE technique. It consists of (i) a 500-nm-thick n-InP cladding layer, (ii) a 30-nm-thick n-AlInAs layer, (iii) five 1.4% compressively strained (CS) $Al_{0.15}Ga_{0.12}In_{0.73}As$ quantum-wells (5QWs, 5-nm-thick for 1.3 μm wavelength) with 10-nm-thick −0.7% tensile-

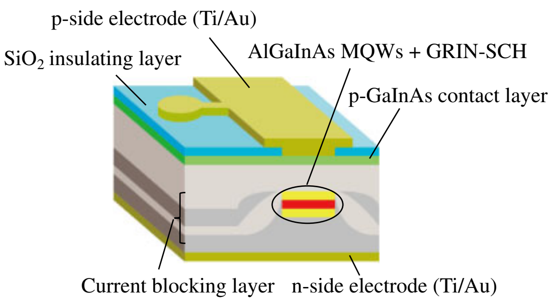

Fig. 1. (Color online) Structure of the fabricated BH lasers.

strained (TS) $Al_{0.25}Ga_{0.32}In_{0.43}As$ barrier layers sandwiched between 100-nm-thick AlGaInAs graded-index separate-confinement-heterostructure (GRIN-SCH) layers, (iv) a 30-nm-thick p-AlInAs layer, (v) a 30-nm-thick p-InP layer, and (vi) a 30-nm-thick GaInAs layer.

Using a SiO_2 mask, mesas of various widths (2, 3, 5, 7, 10, 20, and 50 μm) were formed by wet and dry etching. First, the GaInAs and the Al-containing layers (about 450 nm thick) were etched by a bromomethane solution ($Br_2/CH_3OH = 1 : 1000$) to reach the n-InP cladding layer. After etching, the actual mesa stripes narrowed by approximately 1.4 μm compared with the original mask since the etching process is isotropic. Second, additional etching to the depth of 300 nm was achieved by CH_4/H_2 reactive-ion etching (RIE). This was followed by wet cleaning with $Br_2/CH_3OH = 1 : 40000$, $H_2SO_4/H_2O_2/H_2O = 1 : 1 : 40$, and 1% BHF to clean the entire surface and the Al-containing region, and to remove the oxidized layer, respectively. Then, the wafer was immediately loaded into the OMVPE reactor and exposed to thermal cleaning in a PH_3 atmosphere to expose a fresh regrowth surface prior to the growth of current-blocking layers. In this process, the reactor temperature was fixed at 450 °C on the basis of the results of our initial experiment with various cleaning temperatures ranging from 250 °C to 450 °C. The lasing characteristics of devices prepared at a cleaning temperature of 250 °C, which is the temperature for GaInAsP/InP regrowth, were found to be poor compared with those obtained from devices prepared at a cleaning temperature of 450 °C. Cleaning times of 15, 30, 45, 60, and 90 min were used. Current-blocking layers consisting of 100-nm-thick n-

*E-mail address: n-nishi@pe.titech.ac.jp

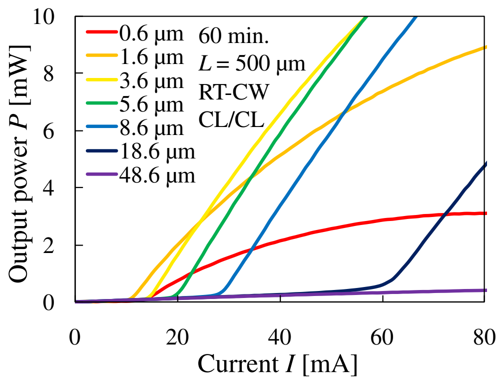

Fig. 2. (Color online) I–P characteristics for 60 min cleaning ($L = 500\,\mu\text{m}$).

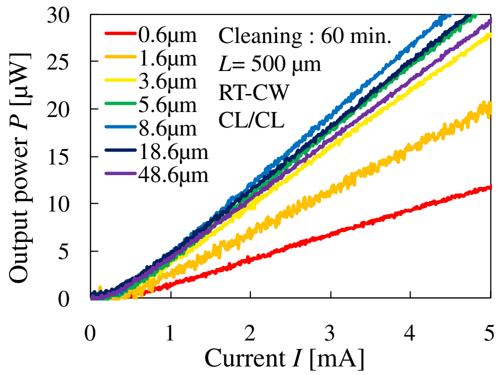

Fig. 3. (Color online) Detailed view of I–P characteristics below threshold for 60 min cleaning ($L = 500\,\mu\text{m}$).

InP, 200-nm-thick p-InP, and 300-nm-thick n-InP were selectively grown to bury the mesa stripes. After removing the SiO_2 mask and the GaInAs layer, the wafer underwent the second regrowth of a 1.6-µm-thick p-InP cladding layer and a 50-nm-thick p^+-GaInAs contact layer. After polishing the substrate, Ti/Au electrodes were evaporated and laser cavities were formed by cleavage.

Figure 2 shows the I–L characteristics under a room temperature continuous-wave (RT-CW) operation for various stripe-width devices with a cavity length of 500 µm and subjected to a 60-min cleaning process, and Fig. 3 shows a detailed view of the I–L characteristics below the threshold. The lasing wavelength was 1.34 µm. The threshold current I_{th}, threshold current density J_{th}, and external differential quantum efficiency η_{d} for various stripe widths are listed in Table I. CW operation was not obtained for the device with a stripe width of 48.6 µm because these devices were not bonded to the heatsinks.

Since J_{th} decreased with stripe width and η_{d} was considerably reduced at stripe widths of less than 1.6 µm, this tendency can be attributed to non radiative recombination at the regrowth interface. We evaluated the sidewall recombination velocity S using[15]

$$\frac{\eta_{\text{spon,BH}}}{\eta_{\text{spon,BH0}}} = 1 - \frac{\dfrac{2S\cdot\tau}{W - 2W_{\text{d}}}}{1 + \dfrac{S\cdot\tau}{L_{\text{D}}}\coth\left(\dfrac{W - 2W_{\text{d}}}{2L_{\text{D}}}\right)}, \qquad (1)$$

Table I. Stripe width dependence of fundamental lasing properties ($L = 500\,\mu\text{m}$).

Stripe width W (µm)	Threshold current I_{th} (mA)	Threshold current density J_{th} (A/cm^2)	External differential quantum efficiency η_{d} (%)
0.6	12.9	4300	22
1.6	9.5	1188	39
3.6	13.9	772	55
5.6	19.3	689	63
8.6	27.7	644	58
18.6	58.8	632	48

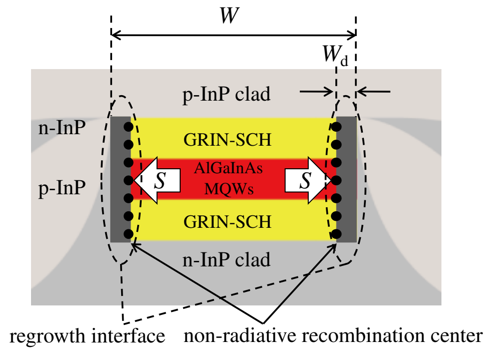

Fig. 4. (Color online) Cross-sectional structure around the active region.

where $\eta_{\text{spon,BH}}$ is the spontaneous emission efficiency (measured from Fig. 3) at a low injection current level; τ is the carrier lifetime of the BH structure when $S = 0$; L_{D} is the diffusion length, which is 5 µm in AlGaInAs;[16] W is the stripe width; and W_{d} is the "dead layer thickness[17]". However, in this study, we have assumed W_{d} to be negligible as $W \gg W_{\text{d}}$ because the W_{d} considered as the lattice defect region owing to the oxidation of Al-containing layers was found to be very thin from our TEM measurements. Furthermore, $\eta_{\text{spon,BH0}}$ is the spontaneous emission efficiency of the 48.6-µm-wide-stripe BH laser with the same cleaning time for normalization. Figure 4 shows the cross-sectional structure of the active region and the regrowth interface. If there are no non radiative recombination centers at the regrowth interface, which corresponds to $S\cdot\tau = 0$, the normalized spontaneous emission efficiency $\eta_{\text{spon,BH}}/\eta_{\text{spon,BH0}}$ should approach a value of 1 even for a narrow stripe width.

Figure 5 shows the normalized spontaneous emission efficiency of BH lasers with a cavity length L of 500 µm as a function of the stripe width. From these data and eq. (1), the $S\cdot\tau$ product was estimated, by the least-squares method, to be 619 (poor fitting), 307, 315, 343, and 1723 nm for cleaning time periods of 15, 30, 45, 60, and 90 min, respectively. However, in the case of the 15-min cleaning process, the $\eta_{\text{spon,BH}}/\eta_{\text{spon,BH0}}$ value did not reach 1 even for wide-stripe (e.g., 8.6 or 18.6 µm) samples because of the large non-radiative recombination components observed throughout the stripe, not only at the side walls of the stripe. Thus clear improvement was observed for the cleaning time range from 30 to 60 min compared with 15 and 90 min.

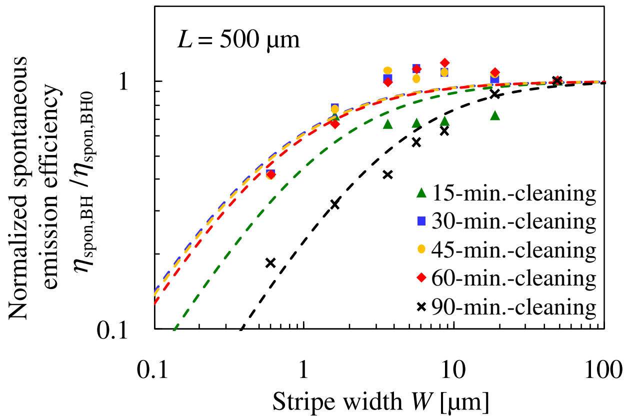

Fig. 5. (Color online) Stripe-width dependence of normalized spontaneous emission efficiency.

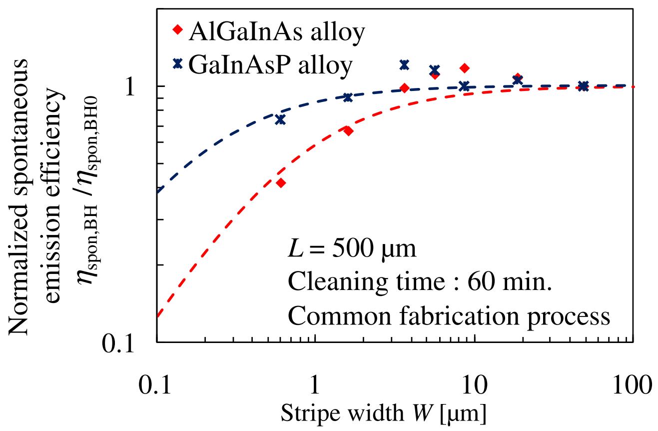

Fig. 6. (Color online) $S \cdot \tau$ products for AlGaInAs with GaInAsP.

Furthermore, the $S \cdot \tau$ product of the AlGaInAs/InP alloy system was compared with that of the GaInAsP/InP system, as shown in Fig. 6. Devices made of the GaInAsP/InP system were fabricated by the same etching, cleaning, and regrowth processes as used for the AlGaInAs/InP BH lasers (60 min cleaning). Please note that the lasing wavelength for this GaInAsP/InP system was the 1.55 µm band. The $S \cdot \tau$ product of this system was estimated to be 80 nm, which is close to the previously reported value.[18] Although our AlGaInAs/InP BH laser characteristics are comparable to those mentioned in other reports,[8,9] the $S \cdot \tau$ product of the present AlGaInAs/InP BH structure is still 5 times larger than that reported for the GaInAsP/InP system. Therefore, there is plenty of room for further improvement in the non radiative recombinations at the regrowth interface.

Finally, we estimated the internal quantum efficiency η_i and the waveguide loss α_{WG} from the cavity length dependence on the inverse of the external differential quantum efficiency η_d (both facets) of lasers with the stripe width of 3.6 µm. The values are listed in Table II. It is significant to note that that appropriate thermal cleaning time periods in the range of 30 to 60 min lead to higher η_i values and hence improved lasing characteristics; this tendency is also compatible with observations made in the evaluation of sidewall recombination velocity.

Table II. Cleaning time dependence of internal quantum efficiency and waveguide loss ($W = 3.6$ µm).

	Cleaning time (min)				
	15	30	45	60	90
Internal quantum efficiency η_i (%)	57	67	75	65	43
Waveguide loss α_{WG} (cm^{-1})	6	4	5	4	7

In conclusion, AlGaInAs/InP BH lasers were fabricated and their regrowth interface quality was investigated in terms of the non radiative recombination rate at the regrowth interfaces. The quantitative study of the regrowth interface revealed that proper thermal cleaning is essential, and an internal quantum efficiency as high as 75% and waveguide loss of 5 cm^{-1} with a stripe width of 3.6 µm were achieved.

Acknowledgements We would like to thank Professors Emeriti Y. Suematsu and K. Iga for their continuous encouragement, and Professors M. Asada, F. Koyama, T. Mizumoto, Y. Miyamoto, and M. Watanabe of the Tokyo Institute of Technology for the fruitful discussions. This research was partially supported by Grants-in-Aid for Scientific Research (19002009, 21226010, 21860031, 22360138, and 10J09593) from the Ministry of Education, Culture, Sports, Science and Technology, Japan (MEXT).

1) C. E. Zah, R. Bhat, B. N. Pathak, F. Favire, W. Lin, M. C. Wang, N. C. Andreadakis, D. M. Hwang, M. A. Koza, T. P. Lee, Z. Wang, D. Darby, D. Flanders, and J. J. Hsieh: IEEE J. Quantum Electron. **30** (1994) 511.
2) R. F. Kazarinov and G. L. Belenky: IEEE J. Quantum Electron. **31** (1995) 423.
3) M. Kubota, K. Hamano, K. Takemasa, M. Kobayashi, H. Wada, and T. Munakata: Jpn. J. Appl. Phys. **39** (2000) 2297.
4) M. Allovon and M. Quillec: Proc. IEE **139** (1992) 148.
5) J. C. L. Yong, J. M. Rorison, and I. H. White: IEEE J. Quantum Electron. **38** (2002) 1553.
6) T. J. Houle, J. C. L. Yong, C. M. Marinelli, S. Yu, J. M. Rorison, I. H. White, J. K. White, A. J. SptingThorpe, and B. Garrett: IEEE J. Quantum Electron. **41** (2005) 132.
7) T. Tanbun-Ek, S. N. G. Chu, P. W. Wisk, R. Pawelek, A. M. Sergent, J. Minch, E. Young, and S. L. Chuang: in Proc. 10th Int. Conf. Indium Phosphide and Related Materials, 1998, p. 702.
8) K. Takemasa, M. Kubota, T. Munakata, and H. Wada: IEEE Photonics Technol. Lett. **11** (1999) 949.
9) T. Nakamura, T. Okuda, R. Kobayashi, Y. Muroya, K. Tsuruoka, Y. Ohsawa, T. Tsukuda, and S. Ishikawa: IEEE J. Sel. Top. Quantum Electron. **11** (2005) 141.
10) K. Yashiki, T. Kato, H. Chida, K. Tsuruoka, R. Kobayashi, S. Sudo, K. Sato, and K. Kudo: IEEE Photonics Technol. Lett. **18** (2006) 109.
11) K. Otsubo, M. Matsuda, K. Takada, S. Okumura, M. Ekawa, H. Tanaka, S. Ide, K. Mori, and T. Yamamoto: Electron. Lett. **44** (2008) 631.
12) N. Ikoma, T. Kawahara, N. Kaida, M. Murata, A. Moto, and T. Nakabayashi: Proc. Optical Fiber Communication Conf., 2005, OThu1.
13) R. Gessner, A. Dobbinson, A. Miler, J. Rieger, and E. Veuhoff: J. Cryst. Growth **248** (2003) 426.
14) H. Ichikawa, S. Matsukawa, K. Hamada, N. Ikoma, and T. Nakabayashi: J. Appl. Phys. **106** (2009) 083101.
15) B. E. Maile, A. Forchel, and R. Germann: Appl. Phys. Lett. **54** (1989) 1552.
16) H. Park, A. W. Fang, O. Cohen, R. Jones, M. J. Paniccia, and J. E. Bowers: IEEE J. Sel. Top Quantum Electron. **12** (2006) 1657.
17) D. B. Wittry and D. F. Kyser: J. Appl. Phys. **38** (1967) 375.
18) M. Tamura, T. Ando, N. Nunoya, S. Tamura, S. Arai, and G. U. Bacher: Jpn. J. Appl. Phys. **37** (1998) 3576.

